Computers and Electronics in Agriculture 134 (2017) 19–26

Contents lists available at ScienceDirect

Computers and Electronics in Agriculture

journal homepage: www.elsevier.com/locate/compag

Original papers

Attitude measure system based on extended Kalman filter for multi-rotors

Zhang Tiemin *, Liao Yihua

Key Laboratory of Key Technology on Agricultural Machine and Equipment, Ministry of Education, South China Agricultural University, Guangzhou 510642, China

ARTICLE INFO

Article history:
Received 24 March 2016
Received in revised form 23 October 2016
Accepted 26 December 2016
Available online 19 January 2017

Keywords:
Multi-rotor
Attitude measure
Sensor fusion
Extended Kalman filter
Quaternion

ABSTRACT

Attitude measure is the basis of multi-rotors flight control. An attitude measure system was constructed based on MEMS gyroscope, accelerometer and magnetometer to realize three-axis attitude measure of multi-rotors. The system included STM32F103 as controller, integrated accelerometer and gyroscope MPU6050, magnetometer HMC5883 as measure sensors. A sensor fusion quaternion-based extended Kalman filter compliant with this system was proposed. The attitude quaternion and the gyroscope bias were introduced as state vector, the acceleration and the magnetic measured by accelerometer and magnetometer were introduced as observation vector. Extended Kalman filter combined the nice performance of gyroscope in dynamic with accelerometer and magnetometer in static. The optimized covariance value combination can improve the accuracy of attitude estimation and had excellent tracking performance in dynamic. The measure system based on extended Kalman filter was testified and analyzed by static and dynamic tests. Experiment results illustrated that the system can obtain the information of each sensor. The attitude measure system based on extended Kalman filter realized precision attitude measure for multi-rotors in dynamic circumstances. It may lay foundation for UAV remote control.

0. Introduction

Multi-rotors is being introduced into almost every aspect of life. Agriculture is one such domain where multi-rotors is successfully used to reap numerous benefit. Croplands are extensive, with a size of up to several kilometers. Hence, it is necessary to use multi-rotors to hover and acquire accurate real-time target image to detect water accumulation on plant surface (Lee et al., 2010). Another key point is that it can work on farmland. For example, if a disease is detected, insecticides can be used to against them. Multi-rotors can transport these substances and release them at a particular point when necessary. Aerial remote sensing with high-resolution imaging showed a great potential for detecting disease-infected trees, evaluating the emergence and spring stand of wheat (Sankaran et al., 2015, 2010; Garcia-Ruiz et al., 2013).

Multi-rotors, which usually has more than two rotor propellers, has the advantages of taking off and landing vertically, simple structure, high mobility, good safety and easy maintenance. It is an understable and strong coupling system with 6 freedoms and 4 inputs. Therefore, to improve the vehicle's stability and controllability to make it fly autonomously or be guided manually is very useful. Attitude measure is an important part of the control system in multi-rotors and the accuracy of the measure system impacts control performance significantly. As a result, an attitude measure system needs to be constructed for the multi-rotors. Moreover, it can provide attitude information for UAV remote control operation test system of Zhang et al. (2015).

MEMS (Micro-Electro-Mechanical System) technologies have rapid developed during recent years. It is the high tech electronic mechanical devices that incorporate the technology of lithography, etching, silicon micro process, non silicon micro process and precision mechanics. Pastell et al. (2008) introduced a system, which was composed of electromechanical film, can detect dynamic forces to identify cow's lameness. In addition, the system suitable for attitude measure in multi-rotors has limitations on size, weight and power consumption (Liu et al., 2012; Wu and Yan, 2012). In order to achieve precision measurement, a sensor-integrated algorithm which could process data fusion and be compliant with the proposed hardware system should be researched in this study.

Different fusion algorithms such as Kalman filter, complementary filter, gradient descent method have been implemented in sensor-integrated systems these years. The gradient descent algorithm was provided in literature of Peng et al. (2015). Liao et al. (2014) had developed a multi-sensor data fusion method with fuzzy-PI deviation correction based on quaternion attitude system.

* Corresponding author.
E-mail address: tiemin_zhang@sina.com (T. Zhang).

http://dx.doi.org/10.1016/j.compag.2016.12.021
0168-1699/

While there are multiple fusion algorithms, Kalman fusion algorithm has been extensively implemented. Kalman filter is a recursive algorithm for efficient estimation of the process subjected to random disturbance based on minimum variance estimation (Xie et al., 2007).

In order to increase the attitude measuring precision, Yang et al. (2012) introduced an extended Kalman Filter (EKF) to integrate attitude data from different sources, however, only simulation results were given. Extended Kalman filter methods for attitude estimation were analyzed in literature of Huang et al. (2005). Gauss-Newton iterative method was employed to calculate the accelerometer and magnetometer vectors as measurement vector. Measure data collected from the sensors were used to test the filter. In the research carried out by Xue et al. (2009), a new quaternion-based extended Kalman filter algorithm by using the modified Gauss-Newton algorithm was introduced to improve the accuracy of attitude estimation. The Kalman filter of Nie et al. (2013) embedded with the gradient descent method was proposed to work out the sensors fusion by using measure information from gyroscope, accelerometer and magnetometer.

Kalman filter adopts recursive algorithm and needs small storage. It not only can be applied in a stationary stochastic process, but also a multi-dimensional and non-stationary random process (Fu et al., 2003). However, few researchers have addressed the problem of realization of attitude system based on extended Kalman filter and illustrated covariance matrices value used in the filter. Therefore, the aim of this work is to create a flight attitude measurement system based on STM32F103 controller, MEMS inertial sensors MPU6050 and HMC5883L. Because the cost of STM32F103, MPU6050 and HMC5883 were $2.1, $5.5 and $1.7 respectively, a low-cost attitude measure system by integrated MEMS sensors to provide accurate attitude measure for UAV became available. The information from gyroscope, accelerometer and magnetometer were integrated by Kalman filter. Extended Kalman filter was adopted because the state matrix and the observation matrix of the system in this paper were nonlinear (Huang and Wang, 2015). In the filter, the quaternion state vector was built from gyroscope and its deviations were corrected by gravity field and magnetic field to estimate the attitude of multi-rotors.

The remainder of this paper is organized as follows. The definition of coordinates and the mathematical basis of the quaternion and its conversions are presented in Section 1. Section 2 is dedicated to the mathematical formulation of extended Kalman filter identification approach and its utilization in the measure system. The experimental setups in this research are described in Section 3. The results of covariance matrices value combinations in this system and the static and dynamic performance based on these combinations are also presented in this section. At the end of Section 4, the discussions and conclusions of this research are presented.

1. Coordinate and quaternion matrix definition

As indicated in Fig. 1, the navigation coordinate system n applied in this paper is North-East coordinate. The body coordinate system b is fixed to the origin of multi-rotors, Ox_b points to the front, Oy_b points to the right while Oz_b points to below. The pitch angle θ of aircraft is between Ox_b axis and ground level, the roll angle φ is between Oz_b axis and the vertical plane Ox_b axis lies in, the heading angle ψ is between the Ox_b axis of aircraft and the North.

Euler angle, direction cosine and quaternion have been the definition methods of orientation in attitude measure system by far. In attitude estimate, the measure vectors from body coordinate can be converted to navigation coordinate by coordinate conversion matrix C_b^n. In Euler angle, the representation of conversion matrix C_b^n is defined by

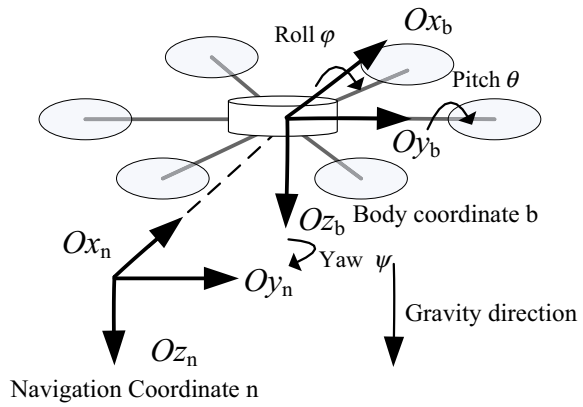

Fig. 1. Navigation coordinate and body coordinate of multi-rotors.

$$C_b^n = \begin{pmatrix} \cos\varphi\cos\psi + \sin\varphi\sin\theta\sin\psi & \cos\theta\sin\psi & \sin\varphi\cos\psi - \cos\varphi\sin\theta\sin\psi \\ -\cos\varphi\sin\psi + \sin\varphi\sin\theta\cos\psi & \cos\theta\cos\psi & -\sin\varphi\sin\psi - \cos\varphi\sin\theta\cos\psi \\ -\sin\varphi\cos\theta & \sin\theta & \cos\varphi\cos\theta \end{pmatrix}. \tag{1}$$

Attitude estimation resolved by quaternion can reduce computation and avoid singularity problem of Euler angle. The expression of quaternion is $\boldsymbol{q} = [q_0\ q_1\ q_2\ q_3]^{\mathrm{T}}$. In quaternion, body coordinate can be achieved by continuous rotation conversions of navigation coordinate without interruption. Inverse matrix of conversion matrix is the transposition of itself. Quaternion coordinate conversion matrix from navigation coordinate to body coordinate is,

$$C_n^b(\vec{q}) = \begin{bmatrix} q_0^2+q_1^2-q_2^2-q_3^2 & 2(q_1q_2+q_0q_3) & 2(q_1q_3-q_0q_2) \\ 2(q_1q_2-q_0q_3) & q_0^2-q_1^2+q_2^2-q_3^2 & 2(q_2q_3+q_0q_1) \\ 2(q_1q_3+q_0q_2) & 2(q_2q_3-q_0q_1) & q_0^2-q_1^2-q_2^2+q_3^2 \end{bmatrix}. \tag{2}$$

Combining Eqs. (1) and (2) yields attitude angle as follows,

$$\begin{cases} \theta = \arcsin\left((C_n^b(\vec{q}))_{23}\right), [\frac{\pi}{2}, \frac{\pi}{2}] \\ \phi = -\arctan\left(\frac{(C_n^b(\vec{q}))_{13}}{(C_n^b(\vec{q}))_{33}}\right), [-\pi, \pi]. \\ \psi = \arctan\left(\frac{(C_n^b(\vec{q}))_{21}}{(C_n^b(\vec{q}))_{22}}\right), [-\pi, \pi] \end{cases} \tag{3}$$

In strap-down inertial navigation system, the relationship between angular velocity and unit quaternion is as follow,

$$\begin{bmatrix} \dot{q}_0 \\ \dot{q}_1 \\ \dot{q}_2 \\ \dot{q}_3 \end{bmatrix} = \frac{1}{2}\begin{bmatrix} 0 & -\omega_x & -\omega_y & -\omega_z \\ \omega_x & 0 & \omega_z & -\omega_y \\ \omega_y & -\omega_z & 0 & \omega_x \\ \omega_z & \omega_y & -\omega_x & 0 \end{bmatrix}\begin{bmatrix} q_0 \\ q_1 \\ q_2 \\ q_3 \end{bmatrix}, \tag{4}$$

where ω_x, ω_y, ω_z are the real rotation rates around x, y, z axis in the body coordinate measured by gyroscope (Qin et al., 1998).

2. Attitude estimation in Kalman filter

2.1. Kalman filter

MEMS gyroscope has very fast dynamic response and great accuracy except for errors which composes drift bias and white noise. The raw data from gyroscope cannot be used directly, because it infiltrates drift bias over time. In addition, it does not provide an absolute angle since the angle information from gyroscope is a relative angle from the initial point. The accelerometer has high accuracy in static. But it is influenced by acceleration motion and cannot restrain high dynamic maneuvers. Magnetome-

ter is sensitive to the interference of external magnetic field which affects measurement accuracy. Therefore, the attitude information obtained separately by each sensors cannot satisfy the precision of flight control. Appropriate algorithm which can integrate MEMS-based sensors to calibrate and estimate attitude is indispensable (Zhang et al., 2011; Du et al., 2010; Wu and Bao, 2010). As a result, the quaternion-based extended Kalman filter which can combine agility of gyroscope and stability of accelerometer and magnetometer is adopted to gain real-time optimized attitude estimation.

Kalman filter algorithm is a discrete time algorithm. The model of a linear time invariant discrete system implement Kalman filter is given in

$$\begin{aligned} x(k+1) &= \phi x(k) + w(k) \\ z(k) &= hx(k) + v(k) \end{aligned} \tag{5}$$

Eq. (5) defines the state and the observation processes. The matrix ϕ governs the transition of the state vector x from time k to time $k+1$. The observation matrix h relates the observation vector z to the state vector x. w and v represent the process noise vector and the measure noise vector. They are assumed to be zero mean white noise. The overall structure of Kalman filter is given in Fig. 2.

2.2. Extended Kalman filter

To implement Kalman filter in multi-sensors fusion, the gravity field and the magnetic field as the reference vectors have to be computed. The normalized gravity vector $\boldsymbol{g}_n$ and the magnetic field $\boldsymbol{m}_n$ in navigation coordinate are described by $\boldsymbol{g}_n = [0\ 0\ g]^T$ and $\boldsymbol{m}_n = [m_{nx}\ m_{ny}\ m_{nz}]^T$, where g represents gravity acceleration, m_{nx}, m_{ny}, m_{nz} represent the three-axis components of magnetic field vector.

The measures of accelerometer and magnetometer respect to body coordinate are $\boldsymbol{a}_b = [a_x\ a_y\ a_z]^T$ and $\boldsymbol{m}_b = [m_x\ m_y\ m_z]^T$, where a_x, a_y, a_z compose the tri-axial acceleration vector while m_x, m_y, m_z constitute the tri-axial magnetic field vector. Through the quaternion coordinate conversion matrix, $\boldsymbol{g}_n$ and $\boldsymbol{m}_n$ in navigation system can convert to $\boldsymbol{g}_b$ and $\boldsymbol{m}_b$ in body system.

The state vector $\boldsymbol{x}$ including attitude described in unit quaternion and gyroscope bias $\boldsymbol{b}_\omega$ becomes $\boldsymbol{x} = [q_0\ q_1\ q_2\ q_3\ b_{\omega x}\ b_{\omega y}\ b_{\omega z}]^T$. We have the state transition matrix $\boldsymbol{\phi}$ and the observation matrix $\boldsymbol{h}$ as follow,

$$\phi = \frac{1}{2}\begin{bmatrix} 0 & -\omega_x & -\omega_y & -\omega_z \\ \omega_x & 0 & \omega_z & -\omega_y \\ \omega_y & -\omega_z & 0 & \omega_x \\ \omega_z & \omega_y & -\omega_x & 0 \end{bmatrix}\begin{bmatrix} q_0 \\ q_1 \\ q_2 \\ q_3 \end{bmatrix}, \tag{6}$$

$$h = \begin{pmatrix} g_b \\ m_b \end{pmatrix} = \begin{pmatrix} \hat{C}_n^b(k,k-1) & 0 \\ 0 & \hat{C}_n^b(k,k-1) \end{pmatrix}\begin{pmatrix} g_n \\ m_n \end{pmatrix}. \tag{7}$$

Due to the drift bias of gyroscope in the attitude measure, the relation between the real value $\boldsymbol{\omega}$ and the measure value $\boldsymbol{\omega}_m$ is $\boldsymbol{\omega} = \boldsymbol{\omega}_m - \boldsymbol{b}_\omega$.

As formula (6) and (7) shown above, the state matrix and the observation matrix of the attitude measure system in this paper are nonlinear. When the state or the observation equation of the system is nonlinear, Kalman filter cannot be directly applied (Wang et al., 2012). Extended Kalman filter uses the local linear characteristics of the nonlinear function to make Kalman filter is applicable to nonlinear systems (Huang and Wang, 2015; Wang et al., 2011). When a nonlinear system apply Kalman filter, it needs transform into a linear function. Therefore extended Kalman filter is the linearization of a nonlinear system by using Taylor expansion with Jacobian omitted second and higher order items and using the basic steps of Kalman filter to update the estimation. The linearization results in above equations are their Jacobian matrices. They are described as follow,

$$\dot{\Phi} = \frac{\partial\phi}{\partial x} = \frac{1}{2}\begin{bmatrix} 0 & -(\omega_{mx}-b_{\omega x}) & -(\omega_{my}-b_{\omega y}) & -(\omega_{mz}-b_{\omega z}) & q_1 & q_2 & q_3 \\ \omega_{mx}-b_{\omega x} & 0 & \omega_{mz}-b_{\omega z} & -(\omega_{my}-b_{\omega y}) & -q_0 & q_3 & -q_2 \\ \omega_{my}-b_{\omega y} & -(\omega_{mz}-b_{\omega z}) & 0 & \omega_{mx}-b_{\omega x} & -q_3 & -q_0 & q_1 \\ \omega_{mz}-b_{\omega z} & \omega_{my}-b_{\omega y} & -(\omega_{mx}-b_{\omega x}) & 0 & q_2 & -q_1 & -q_0 \\ 0 & 0 & 0 & 0 & 0 & 0 & 0 \\ 0 & 0 & 0 & 0 & 0 & 0 & 0 \\ 0 & 0 & 0 & 0 & 0 & 0 & 0 \end{bmatrix}, \tag{8}$$

$$H = \frac{\partial h}{\partial x} = \begin{bmatrix} \frac{\partial(C_b^n \cdot g_n)}{\partial x}, 0_{3\times3} \\ \frac{\partial(C_b^n \cdot b_n)}{\partial x}, 0_{3\times3} \end{bmatrix} = \begin{bmatrix} H_{a1} & H_{a2} & H_{a3} & H_{a4} & \\ H_{a4} & -H_{a3} & H_{a2} & -H_{a1} & 0_{3\times3} \\ -H_{a3} & -H_{a4} & H_{a1} & H_{a2} & \\ H_{b1} & H_{b2} & H_{b3} & H_{b4} & \\ H_{b4} & -H_{b3} & H_{b2} & -H_{b1} & 0_{3\times3} \\ -H_{b3} & -H_{b4} & H_{b1} & H_{b2} & \end{bmatrix}, \tag{9}$$

where $\begin{cases} H_{a1} = -2q_2g \\ H_{a2} = 2q_3g \\ H_{a3} = -2q_0g \\ H_{a4} = 2q_1g \end{cases}, \begin{cases} H_{b1} = 2(m_{nx}q_0 + m_{ny}q_3 - m_{nz}q_2) \\ H_{b2} = 2(m_{nx}q_1 + m_{ny}q_2 + m_{nz}q_3) \\ H_{b3} = 2(-m_{nx}q_2 + m_{ny}q_1 - m_{nz}q_0) \\ H_{b4} = 2(-m_{nx}q_3 + m_{ny}q_0 + m_{nz}q_1) \end{cases}.$

Considering operation speed of the system hardware and extended Kalman filter structure, Lagrange method is implemented in the state matrix as discrete time linearization approximations. The state equation is transformed as follow, T is the period of update interval,

$$\Phi = I + \dot{\Phi}T = I + \frac{\partial\phi}{\partial x}T. \tag{10}$$

The block diagram of extended Kalman filter applied in attitude estimation process is illustrated as follow (see Fig. 3).

Extended Kalman filter functions in a predict fashion. The prediction $\hat{x}(k+1,k)$ is propagated in first by propagating the old estimate $\hat{x}(k)$ through the state matrix at time step k as follow,

$$\hat{x}_{7\times1}(k+1,k) = \Phi_{7\times7}\hat{x}_{7\times1}(k). \tag{11}$$

In order to represent the reliability of state estimate $\hat{x}$, its error covariance $\boldsymbol{P}$ is maintained by

$$P_{7\times7}(k+1,k) = \Phi_{7\times7}P_{7\times7}(k)\Phi_{7\times7}^T + Q_{7\times7}. \tag{12}$$

where $\boldsymbol{Q}$ is the covariance matrix of process noise w.

Then the prediction $\hat{x}(k+1,k)$ can be improved by incorporating observations of accelerometer and magnetometer. These observations may be incorporated to give corrected estimate $\hat{x}(k+1)$ as follow,

$$\begin{aligned} K_{7\times6}(k+1) &= P_{7\times7}(k+1,k)H_{7\times6}^T(k+1)[H_{6\times7}(k+1)P_{7\times7}(k+1,k) \\ &\quad \times H_{7\times6}^T(k+1) + R_{6\times6}]^{-1} \\ \hat{x}_{7\times1}(k+1) &= \hat{x}_{7\times1}(k+1,k) + K_{7\times6}(k+1)[z_{6\times1}(k+1) \\ &\quad - H_{6\times7}(k+1)\hat{x}_{7\times1}(k+1,k)] \\ P_{7\times7}(k+1) &= [I_{7\times7} - K_{7\times6}(k+1)H_{6\times7}(k+1)]P_{7\times7}(k+1,k) \end{aligned} \tag{13}$$

where $\hat{x}(k+1)$ is the updated estimate state. The process noise vector w, is assumed to be white noise and have a noise covariance

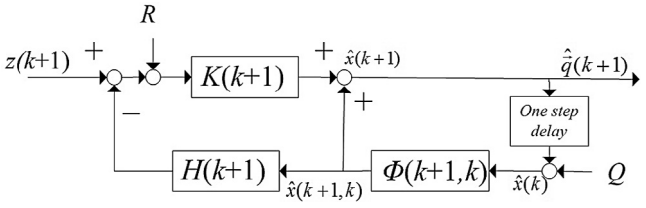

Fig. 2. Kalman filter structure for a linear discrete system.

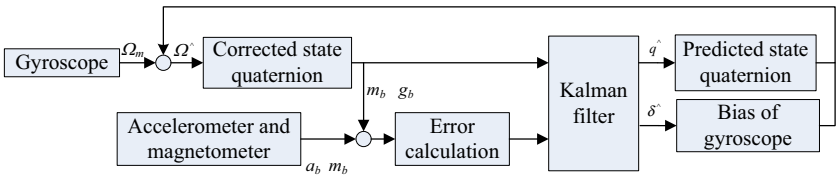

Fig. 3. The block diagram of extended Kalman filter in attitude estimation.

matrix $\boldsymbol{Q}$. The measurement noise vector v, is assumed to be white noise and have a noise covariance matrix $\boldsymbol{R}$.

$\boldsymbol{P}(k+1)$ is covariance matrix of estimate error. $\boldsymbol{P}(k+1)$ is known as the information matrix measuring the accuracy of estimated $\hat{x}(k+1)$, which is the integrated information provided by state prediction and sensors observation. Therefore the third equation of Eq. (13) combines the state prediction with the new sensors observations. The size of each matrix in extended Kalman filter is specified by their subscript.

$\boldsymbol{K}(k+1)$ is the Kalman filter gain. $\boldsymbol{H}$ is the Jacobian of the observations matrix at time step $k+1$, $\boldsymbol{z}(k+1)$ is the observation vector composed of acceleration measure vector and magnetic measure vector, which are $\boldsymbol{a}_b = [a_x\ a_y\ a_z]^T$ and $\boldsymbol{m}_b = [m_x\ m_y\ m_z]$, measured by accelerometer and magnetometer in body fame. Hence, Kalman filter can fulfill the sensor fusion procedure to find the optimized estimate quaternion by relating measure vectors in the body frame and reference vectors in the navigation frame. Fig. 4 is the calculation flow chart of estimate error covariance $\boldsymbol{P}$ and the state vector $\boldsymbol{x}$.

3. Experiment analysis and results

The attitude measure system contains STM32F103 as controller, MPU6050 (InvenSense Co., America) as tri-axial gyroscope and tri-axial accelerometer, HMC5883 (Honeywell Co., America) as tri-axial magnetometer. The gyroscope has ±250/500/1000/2000°/s measure range and the accelerometer has 4/+8/+2/+16 g measure range. The output data of MPU6050 are obtained from 16 bit analog/digital converter. The magnetometer has 13 bit output data with 1200 μT measure range. The power of sensors are supplied by the controller and communicated with it by I2C interface. The hardware structure of the attitude measure system is illustrated in Fig. 5.

3.1. Covariance tunings

The system go through sensors fusion procedure to acquire attitude estimation. In the prediction step of EKF, the accelerometer and magnetometer measurements are used to predict the growth of estimate error covariance matrix $\boldsymbol{P}$. $\boldsymbol{P}$ means the confidence of the estimated state process. By including other sensors in feedback loop, estimate error covariance can be reduced in the correction steps and estimate the true error. The sensors are sampled in discrete time with 115 Hz. The noise of each sensor is independent. They are random and have no relationship with sampling time (Schinstock, 2014). The process noise covariance matrix $\boldsymbol{Q}$ and the observation noise covariance matrix $\boldsymbol{R}$ are diagonal matrices. The covariance matrices need to be adjusted to improve the filter convergence.

As an initial value for $\boldsymbol{P}_k$, $\boldsymbol{P}_0$, needs to be adjusted. Because when the initial estimate state $\hat{x}_0 \neq 0$, choosing $\boldsymbol{P}_0 = 0$ would make the filter initially and always consider $\hat{x}_0 = 0$. As a result, as long as

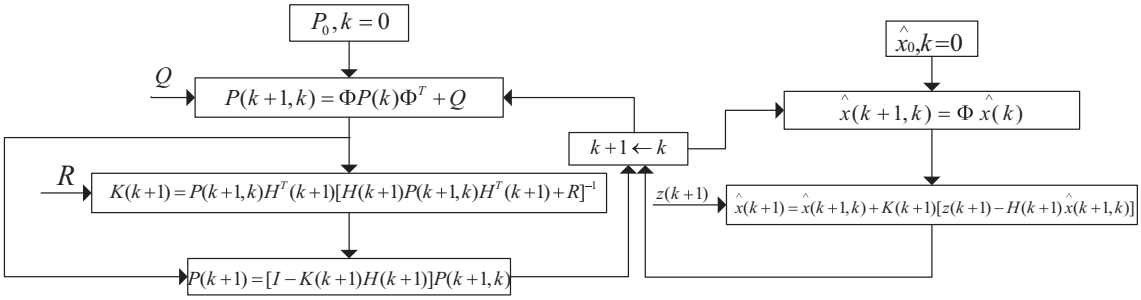

Fig. 4. Flowchart of $\boldsymbol{P}$ and $\boldsymbol{x}$ in prediction step and correction step of Kalman filter.

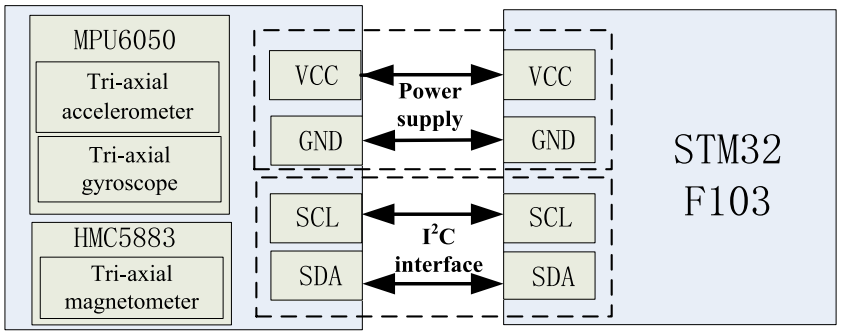

Fig. 5. Hardware structure of the attitude measure system.

$\boldsymbol{P}_0 \neq 0$, the filter would eventually converge (Greg and Gary, 2009). Notice that the error covariance $\boldsymbol{P}$ of the model is uncertainty, the choice for $\boldsymbol{P}_0$ were $0.001 \times \boldsymbol{I}_{7\times7}$, $0.0001 \times \boldsymbol{I}_{7\times7}$, $0.00001 \times \boldsymbol{I}_{7\times7}$.

Because the process signal cannot be directly observed, to determine the $\boldsymbol{Q}$ value is difficult (Wang et al., 2012). $\boldsymbol{Q}$ is assumed to be a very small process variance, almost none. Supposing $\boldsymbol{Q}$ as a small but non-zero value creates flexibility in the filter tuning. Hence $\boldsymbol{Q}$ was defined by $0.001 \times \boldsymbol{I}_{7\times7}$, $0.0001 \times \boldsymbol{I}_{7\times7}$, $0.00001 \times \boldsymbol{I}_{7\times7}$.

$\boldsymbol{R}$ is relevant to the characteristics of the sensors measure, but it cannot be accurately confirmed before filtering. In the research of Greg and Gary (2009), when $\boldsymbol{R} = 1$, the filter response to the measurement is slow. When $\boldsymbol{R} = 0.01$, the filter response to the measurement is accelerated, resulted in increment of measurement variance. When $\boldsymbol{R} = 0.0001$, the filter response to the measurement continues to be quick, which increases measurement variance. Therefore, $\boldsymbol{R}$ was selected as $1 \times \boldsymbol{I}_{6\times6}$, $0.1 \times \boldsymbol{I}_{6\times6}$, $0.01 \times \boldsymbol{I}_{6\times6}$, $0.001 \times \boldsymbol{I}_{6\times6}$, $0.0001 \times \boldsymbol{I}_{6\times6}$.

The essence of Kalman filter is to get the optimal unbiased estimation of the current state by minimum variance theory according to all previous estimation and the current measure. Therefore, the accuracy of the measure data and the choice of measure noise variance $\boldsymbol{R}$ have a great effect on the estimation. The performance of Kalman filter is adjusted according to the process noise covariance matrix $\boldsymbol{Q}$ and the measure noise covariance matrix $\boldsymbol{R}$. $\boldsymbol{Q}$ and $\boldsymbol{R}$ represent the certainty of the error model and the reliability of measurement respectively. The way to find the optimized $\boldsymbol{Q}$ and $\boldsymbol{R}$ value is to adjust their values to get system better estimation performance. The optimized $\boldsymbol{Q}$ and $\boldsymbol{R}$ value in this paper were determined by the following experiment.

After gyroscope, acceleration and magnetometer were corrected by the methods in Liao et al. (2014), the measurement system was placed in level for static measure experiment. As was mentioned above, $\boldsymbol{P}$, $\boldsymbol{Q}$ and $\boldsymbol{R}$ values were selected, the mean square measure error of different combinations of $\boldsymbol{P}$, $\boldsymbol{Q}$ and $\boldsymbol{R}$ values selection are showed in Table 1 and Fig. 6.

As the Table 1 and Fig. 6 shown, the effect of the initial covariance matrix $\boldsymbol{P}_0$ to the filter was quite small. However, to obtain an acceptable transient, the initial condition $\boldsymbol{P}_0$ had to be selected. By choosing a smaller value of $\boldsymbol{Q}$, the transient amplitude would be smaller. Filter convergence became fast and it took less time to achieve the optimal estimation performance. But for $\boldsymbol{R}$, selection of a smaller value caused the risk of divergence. Experimentally we observed the optimized $\boldsymbol{P}$, $\boldsymbol{Q}$, $\boldsymbol{R}$ values combination has the minimum mean square error 0.122. The combination was $\boldsymbol{P} = 0.0001 \times \boldsymbol{I}_{7\times7}$, $\boldsymbol{Q} = 0.0001 \times \boldsymbol{I}_{7\times7}$, $\boldsymbol{R} = 0.001 \times \boldsymbol{I}_{6\times6}$.

3.2. Static test

The measure system was testified by tri-axial SGT320E turntable manufactured by Beijing Aerospace Precision Machinery Institute, China Aviation Industry Corp. With U-O-O structure, the U, O, O shaped frame of the turntable can continuously rotate around the $\boldsymbol{O}z_b$, $\boldsymbol{O}y_b$, $\boldsymbol{O}x_b$ axis infinitely, as Fig. 7 shows. To simulate the orientation transformation on aircraft, the system was mounted on the inner frame. The attitude measure results from the system were compared with the attitude output from the turntable. The attitude angle of the turntable was exported from the high speed serial RS-232 in it with 115,200 bps baudrate.

The control angle of multi-rotors in flight is usually less than 40°. Therefore roll angle static measurements were taken at each 1° when the pitch angle was −40°, −20°, 0°, 20°, 40° separately. Figs. 8 and 9 show the roll angle and its errors measured by the

Table 1
The statistics of mean square errors of $\boldsymbol{P}$, $\boldsymbol{Q}$, $\boldsymbol{R}$ values combinations.

	$\boldsymbol{R}$	$\boldsymbol{P}$ = 0.001				
		1	0.1	0.01	0.001	0.0001
$\boldsymbol{Q}$	0.001	0.257077	0.531649	0.125807	0.179635	6.07
	0.0001	0.158192	0.335178	0.574261	0.132658	0.139676
	0.00001	0.434659	1.007963	1.070862	0.541734	0.124773
				$\boldsymbol{P}$ = 0.0001		
$\boldsymbol{Q}$	0.001	0.141286	0.519308	0.128255	0.147242	6.17
	0.0001	0.263546	0.330739	0.52865	0.121708	0.143762
	0.00001	1.128066	0.992511	0.364556	0.537797	0.149028
				$\boldsymbol{P}$ = 0.00001		
$\boldsymbol{Q}$	0.001	0.481698	0.458496	0.166805	0.459267	2.61
	0.0001	0.307343	0.356858	0.541177	0.504295	0.142361
	0.00001	5.73	0.959931	0.313038	0.496815	0.159917

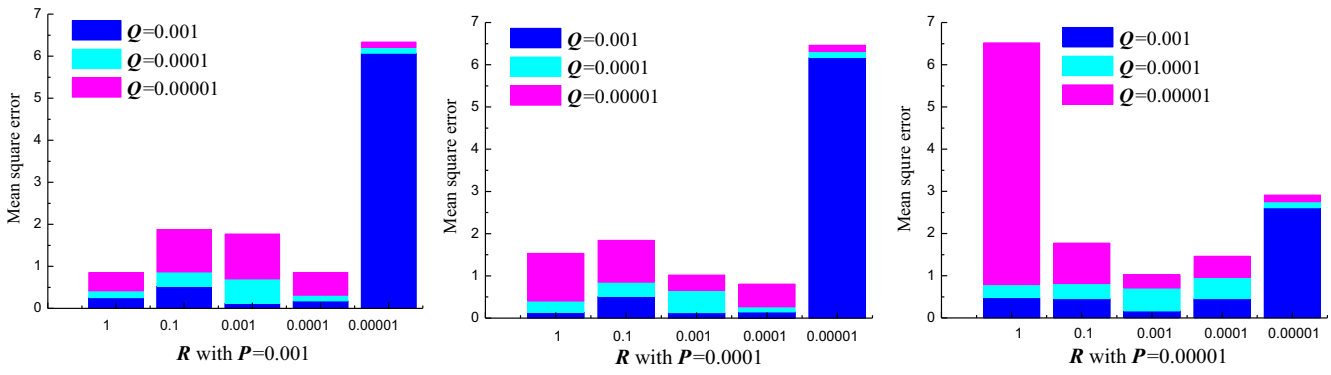

Fig. 6. The histograph of mean square errors of $\boldsymbol{P}$, $\boldsymbol{Q}$, $\boldsymbol{R}$ values combinations.

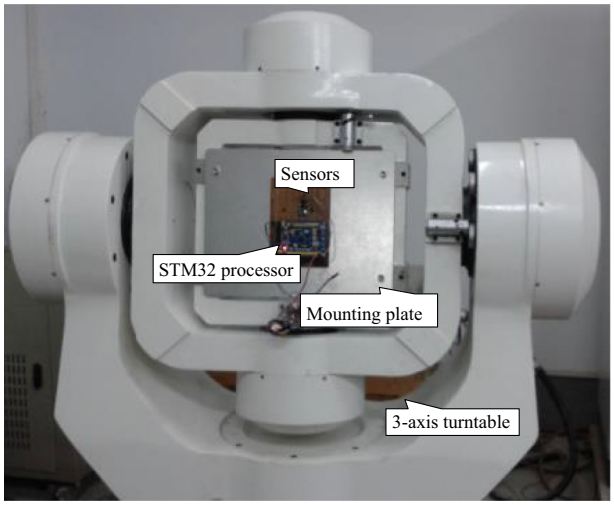

Fig. 7. Attitude measure system on multi-function turntable.

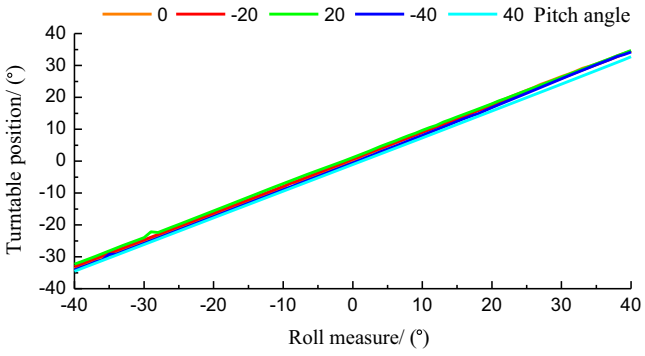

Fig. 8. Static test based on EKF with different pitch angle.

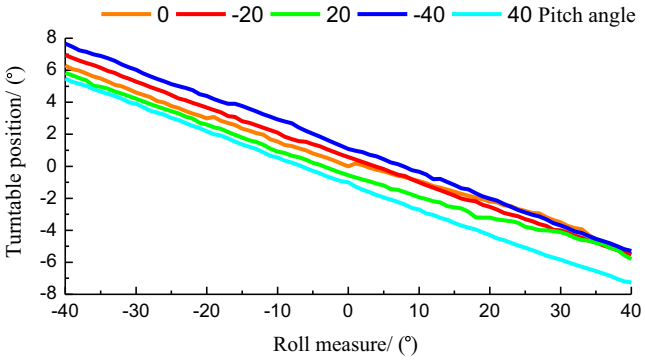

Fig. 9. Errors of static test based on EKF with different pitch angle.

attitude measure system. From the figures below, the error of roll angle increased with the enlargement of pitch angle. The maximum error of roll angle appeared at the largest pitch angle 40°. Moreover, the error near the horizontal was close to 0°.

Fig. 10 shows the static measure of extended Kalman filter-based attitude estimation system with 0° roll angle in a period of time. The attitude measured by the system did not drift or diverge, which demonstrated that appropriate ***P***, ***Q***, ***R*** combination could satisfy static measure requirement and they could estimate accurate attitude. The mean square error in this experiment was 0.122°. The frequency of estimation was recorded by the timer in the controller, which was 115 Hz.

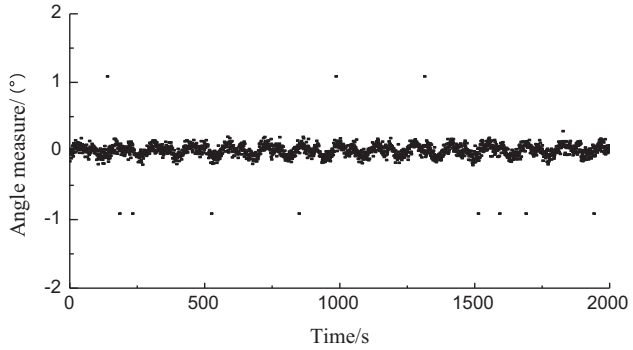

Fig. 10. Static measure in a period of time based on EKF.

3.3. Dynamic test

As multi-rotors makes a various of flight in air, the attitude measure system must have rapid tracking performance to fulfill control task. The dynamic response of the system was testified. The system was mounted on the turntable and the frames of turntable rotated around $\boldsymbol{O}x_b$ axis and $\boldsymbol{O}y_b$ axis in 30° amplitude sine waves with 0.1 Hz. The turntable provided attitude information by high-speed serial port with 10 Hz. Compared the attitude estimated by the measure system with the attitude of turntable, the dynamic tracking performance of this system can be observed. The output attitude estimation of the system and the turntable attitude are presented in Figs. 11 and 12, as well as the measure errors are shown in Figs. 13 and 14.

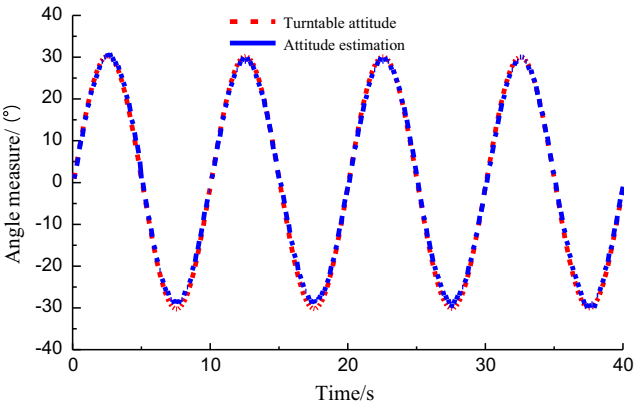

Fig. 11. Dynamic measure based on EKF around the $\boldsymbol{O}x_b$ axis.

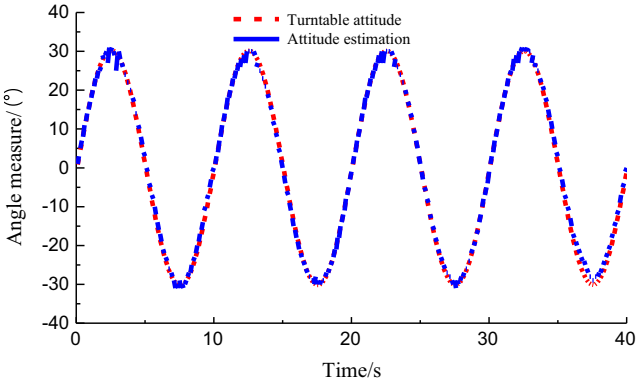

Fig. 12. Dynamic measure based on EKF around the $\boldsymbol{O}y_b$ axis.

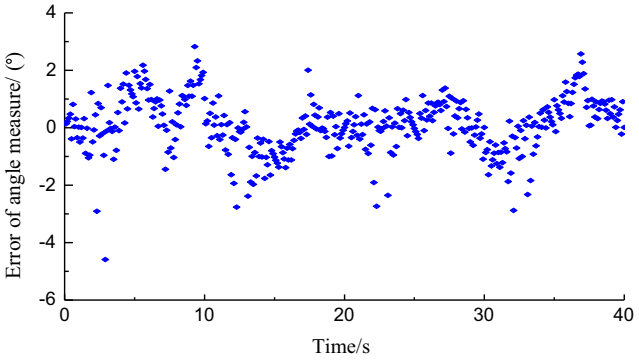

Fig. 13. Errors of dynamic measure based on EKF around the $\boldsymbol{O}x_b$ axis.

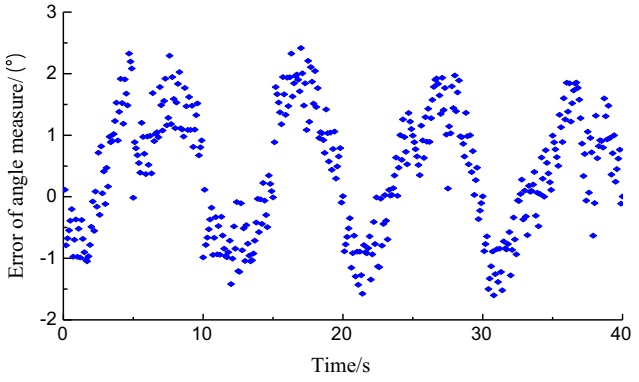

Fig. 14. Errors of dynamic measure based on EKF around the $\boldsymbol{O}y_b$ axiss.

Table 2
The mean absolute errors and the standard errors of the attitude measure system in static and dynamic tests.

	Static measure	Dynamic measure
The mean absolute error of φ/°	3.126	0.432
The standard error of φ/°	3.325	1.078
The mean absolute error of θ/°	3.074	0.107
The standard error of θ/°	3.538	0.963

The statistics of the mean absolute errors and the standard errors of the attitude measure system in static and dynamic tests is summarized in Table 2.

From Figs. 11–14 and Table 2, it could be seen that the deviations of dynamic test were smaller than that of static test with extended Kalman filter. In addition, the mean absolute error of dynamic test was less than 1° in range of ±30°, which proved that the filter with suitable ***P***, ***Q***, ***R*** values combination could estimate the optimal attitude and had superior dynamic tracking performance. Kalman filter has efficient estimation performance. In conclusion, it can satisfy the requirement of attitude angle measure in multi-rotors flight.

4. Conclusion

An attitude measure system applied in multi-rotors composing STM32F103, MPU6050 and HMC5883 was constructed. An extended Kalman filter suitable for multi-sensors fusion based on this system was proposed. The filter used accelerometer and magnetometer measurements as observation vectors to detect and correct errors caused by gyroscope bias to improve measure accuracy. Compared with ***P***, ***Q***, ***R*** covariance matrices different value combinations, the optimized combination was achieved to get more precise measure with the least mean square error.

Experiments showed that the measure errors of the system in static test were less than 3.6°, in dynamic test were less than 1.1°. Moreover, it did not produced static drift or divergence in static test. The frequency of estimation update was 115 Hz. When rotation speed of the turntable was more than 5°/s, the measure system still had rapid tracking characteristics, which proved that the extended Kalman filter proposed in this system had good prediction and correction capability in dynamic test. The attitude measure system has real-time performance to satisfy the multi-rotors attitude control requirement. The sensors employed in the system cost effective, it may be applied in fields more than multi-rotors.

Acknowledgment

This work is supported by the National High Technology Research and Development Program of China (“863” Program) (Grant No. SS2013AA100303) and Open Project of State Key Laboratory of Robotics (Grant No. RL2012-O02).

Appendix A. Supplementary material

Supplementary data associated with this article can be found, in the online version, at http://dx.doi.org/10.1016/j.compag.2016.12.021.

References

Du, J.Y., Huang, G.R., Zhang, F.M., et al., 2010. Design of AHRS based on low-cost MEMS. Chin. J. Sensors Actuat. 23 (11), 1662–1666.
Fu, M.Y., Deng, Z.H., Zhang, J.W., 2003. Kalman Filter Theory and Its Application in Navigation System. China Science Publishing, Beijing.
Garcia-Ruiz, F., Sankaran, S., Maja, J.M., et al., 2013. Comparison of two aerial imaging platforms for identification of Huanglongbing-infected citrus trees. Comput. Electron. Agric. 91, 106–115.
Greg, W., Gary B., 2009. An Introduction to the Kalman Filter, Department of Computer Science University of North Carolina at Chapel Hill. <http://wenku.baidu.com/view/7f52ac02de80d4d8d15a4f07.html>.
Huang, X.P., Wang, Y., 2015. Kalman Filter Principle and Application——MATLAB Simulation. Publishing House of Electronics Industry, Beijing.
Huang, X., Wang, C.H., Yi, G.X., et al., 2005. Extended Kalman filter for IMU attitude estimation using magnetometer, MEMS accelerometer and gyroscope. J. Chin. Inertial Technol. 13 (2), 27–30.
Lee, W.S., Alchanatis, V., Yang, C., et al., 2010. Sensing technologies for precision specialty crop production. Comput. Electron. Agric. 74 (1), 2–33.
Liao, Y.H., Zhang, T.M., Liao, Y.Y., 2014. Multi-rotor aircraft attitude detection system based on fuzzy-proportion integration deviation correction. Trans. Chin. Soc. Agric. Eng. 30 (20), 19–26.
Liu, X.C., Zhang, S., Li, LZ., et al., 2012. Quaternion-based algorithm for orientation estimation from MARG sensors. J. Tsinghua Univ. (Sci & Tech). 52 (5), 627–631.
Nie, P., Li, P.H., Li, Z.H., et al., 2013. Research on attitude measurement system of small drone based on Kalman filter. J. Shenyang Aerospace Univ. 30 (6), 53–57.
Pastell, M., Kujala, M., Aisla, A.-M., et al., 2008. Detecting cow's lameness using force sensors. Comput. Electron. Agric. 64 (1), 34–38.
Peng, X.D., Zhang, T.M., Li, J.Y., et al., 2015. Attitude estimation algorithm of agricultural small-UAV based on sensors fusion and calibration. Acta Automatica Sinica 41 (4), 854–860.
Qin, Y.Y., Zhang, H.Y., Wang, S.H., et al., 1998. Theory of Kalman Filter and Integrated Navigation. Northwestern Polytechnical University Press, Xian City, China, pp. 175–188.
Sankaran, S., Mishra, A., Ehsani, R., 2010. A review of advanced techniques for detecting plant diseases. Comput. Electron. Agric. 72 (1), 1–13.
Sankaran, S., Khot, L.R., Carter, A.H., 2015. Field-based crop phenotyping: Multispectral aerial imaging for evaluation of winter wheat emergence and spring stand. Comput. Electron. Agric. 118, 372–379.
Schinstock, Dale E., 2014. GPS-aided INS Solution for OpenPilot, Kansas State University. <http://wenku.baidu.com/link?url=B7BWMZMyy kw7KtjPu5gttI9Osxw9C8CnVvFYIoCbElUo2gX4mD5Wn_DoSDvBndL2oy1E0bjbLXx3oW9v-gABXGcAa9DNG02wj2Shmx7KMe>.
Wang, S., Tian, B., Zhan, Y.L., Li, Z.F., 2011. Flight attitude estimation for MAVs based on amended EKF. Chin. High Technol. Lett. 21 (6), 612–618.
Wang, X.B., Xu, J.H., Zhang, Zh., 2012. On analysis application approach for Kalman filter parameters. Comput. Appl. Software 29 (6), 212–215.

Wu, J., Bao, Q.L., 2010. Research on high precision optimized strap-down attitude algorithms. Electron. Measure. Technol. 33 (2), 49–52.
Wu, J., Yan, J.G., 2012. Research on attitude estimation algorithm based on Kalman filter. Comput. Simul. 29 (2), 54–57.
Xie, K.M., Li, G.Y., Zheng, D.Z., 2007. Modern Control Theory. Tsinghua University Press, Beijing.
Xue, L., Yuan, W.Z., Chang, H.L., et al., 2009. Application of quaternion-based extended Kalman filter for MAV attitude estimation using MEMS sensors. Nanotechnol. Precision Eng. 7 (2), 163–167.
Yang, S.J., Zeng, Q.S., Yi, G.X., et al., 2012. Study on attitude measuring system on low-cost unmanned aerial vehicle. Transducer Microsyst. Technol. 31 (2), 15–18.
Zhang, H.Q., Zhao, F.Q., Huang, X.Y., et al., 2011. Study on initial alignment of strap-down inertial navigation for land vehicle based on H∞ filter. Foreign Electron. Measure. Technol. 30 (12), 52–55.
Zhang, K., Zhang, T.M., Liao, Y.Y., et al., 2015. Remote control UAV test system based on LabVIEW. Trans. Chin. Soc. Agric. Eng. 31 (S2).